CSF and blood flow patterns in idiopathic normal pressure hydrocephalus

Sara Qvarlander, PhD[1,2] Khalid Ambarki, PhD[1,2] Anders Wåhlin, PhD[1,3] Johan Jacobsson, MD[4] Richard Birgander, MD, PhD[1] Jan Malm, MD, PhD [4] Anders Eklund, PhD[1,2].

[1]Department of Radiation Sciences, Umeå University, Umeå, Sweden.
[2]Centre for Biomedical Engineering and Physics, Umeå University, Umeå, Sweden.
[3]Umeå Centre for Functional Brain Imaging, Umeå University, Umeå, Sweden.
[4]Department of Pharmacology and Clinical Neuroscience, Umeå University, Umeå, Sweden.

Corresponding author:
Sara Qvarlander, Department of Radiation Sciences, Umeå University, SE-90187 Umeå, Sweden. Phone: +46 90 7854152. Email: sara.qvarlander@.umu.se

ABSTRACT

Objectives

Increased aqueduct CSF flow pulsatility, and recently, a reversed CSF flow in the aqueduct have been suggested as hallmarks of idiopathic normal pressure hydrocephalus (INPH). However, these findings have not been adequately confirmed. Our objective was to investigate the flow of blood and CSF in INPH, as compared to healthy elderly, in order to clarify which flow parameters are related to the INPH pathophysiology.

Materials & methods

Sixteen INPH patients (73 years) and 35 healthy subjects (72 years) underwent phase contrast MRI. Measurements included aqueduct and cervical CSF flow, total arterial inflow (tCBF; i.e. carotid + vertebral arteries) and internal jugular vein flow. Flow pulsatility, net flow and flow delays were compared (multiple linear regression, correcting for sex and age).

Results

Aqueduct stroke volume was higher in INPH than healthy (148±95 vs. 90±50 ml, $P<.05$). Net aqueduct CSF flow was similar in magnitude and direction. The cervical CSF stroke volume was lower ($P<.05$). The internal carotid artery net flow was lower in INPH ($P<.05$), though tCBF was not. No differences were found in internal jugular vein flow or flow delays.

Conclusions

The typical flow of blood and CSF in INPH were mainly characterized by increased CSF pulsatility in the aqueduct, and reduced cervical CSF pulsatility. The direction of mean net aqueduct CSF flow was from the third to the fourth ventricle. Our findings may reflect the altered distribution of intracranial CSF volume in INPH, though the causality of these relationships is unclear.

Key words: Aqueduct flow; Cerebral Blood flow; Cerebrospinal fluid; Dementia; Normal pressure hydrocephalus; Phase Contrast Magnetic Resonance Imaging

Introduction

Phase contrast magnetic resonance imaging (PC-MRI) is a promising diagnostic and predictive method to be used in idiopathic normal pressure hydrocephalus (INPH) as it measures flow of blood and CSF in ml/min and is non-invasive. The most consistent finding of previous PC-MRI studies in INPH has been increased cardiac related CSF pulsatility in the aqueduct (1–6). This has been suggested, but not confirmed, as an efficient predictive test for outcome after surgery. It is also unclear if the increase in pulsatility is caused by a reduced intracranial compliance (7) or by an increased ventricular volume (8).

A historic sign of good shunt response was the accumulation of tracer in the ventricles after lumbar injection (radionuclide cisternography) (9,10). A modern equivalent of this has been measurement of direction of the mean flow in the aqueduct: it has been reported that this direction is usually reversed in INPH, i.e., flowing into the ventricles (11,12). These findings have been interpreted as disturbances of the CSF dynamics in INPH and suggested to normalize after CSF diversion. However, few of the PC-MRI studies feature control groups with healthy elderly (1,5,6,13,14), and of those several have employed relatively small and/or non-age-matched control groups or a mix of idiopathic and secondary NPH.

Better predictive tests are needed in the clinical practice of INPH (9). But before putting resources into evaluating new predictive models and tests, such as aqueduct flow and aqueduct CSF pulsatility, it is of importance to understand the pathophysiology behind the new biomarkers. Because disturbance of the CSF flow could be caused by changes in intracranial blood flow, these disturbances may be best understood by taking a comprehensive approach to studying the flow dynamics of INPH, including both the net and pulsatile components of blood flow as well as CSF flow. The aim of the present study was therefore to describe the dynamic pattern of CSF and cerebral blood flow in typical INPH, classified using the INPH guidelines (15), as compared to age-matched healthy elderly.

Material & methods

In summary, 16 INPH patients and 35 healthy volunteers were included and investigated with PC-MRI.

Healthy elderly

Thirty-five healthy elderly subjects were included. Clinical features are shown in Table 1. Healthy elderly were recruited via an advertisement in the local paper and were considered eligible if they did not have any neurological, psychiatric, or advanced vascular diseases. The general selection procedure has previously been reported (16). The age range for inclusion was defined to match a general INPH population and the aim was for 50% female subjects. Data collection took place in parallel with that for suspected INPH subjects, and thus the gender and

age distribution of the final INPH group was not yet clear. To better match the age range of the final INPH group, healthy controls younger than 64 years were excluded in the present study.

Patients

During a 15-month period, patients referred to Umeå university hospital because of communicating hydrocephalus and clinical suspicion of NPH were evaluated for inclusion in the study. Only subjects aged 60-85 years were included. The pre-operative investigation included history, neurological examination, MRI with anatomical and flow sequences, tap test, infusion test and if considered necessary, an external lumbar drainage. Symptoms were quantified using video recordings of gait, evaluation by physiotherapist and Minimental state estimation (MMSE).

We used blinded reviewers for the diagnostic process: two senior neurologists had access to case records (including clinical history, neurological/physical exam and MMSE score) and written reports of the brain MRI investigations, including Evans index. They were not allowed to inspect the MRI scans or results from predictive tests such as infusion test or tap tests. The examiners worked independently of each other and if they had different opinions regarding a patient, the diagnosis was established after discussion. Patients were classified as probable, possible or unlikely INPH based on clinical history, brain imaging and physical findings, according to the international INPH guidelines (15). All patients but one had a normal intracranial pressure (i.e. within 5–18 mm Hg, as defined by the INPH guidelines); this subject was excluded. Subjects classified as unlikely INPH were excluded.

After classification, sixteen INPH patients were included; 12 probable INPH and 4 possible INPH. Clinical features of the two groups are shown in table 1, gender distribution was not perfectly matched in the two groups (healthy: 7 female / 9 male; INPH: 19 female / 16 male) but the proportion of females was not significantly different. Fifteen of the included INPH subjects received a shunt, while 1 subject declined surgery. After shunt surgery, 10 subjects were confirmed to improve (67%), while four revealed little to no improvement. One subject died before follow-up.

Ethical approval

All patients gave informed consent. The Ethical Review board of Umeå University approved the study.

PC-MRI protocol

MRI measurements were performed on a 3T scanner (Achieva, Philips Healthcare, Best, the Netherlands) equipped with an 8-channel head coil; all subjects were investigated with the same scanner. The PC-MRI imaging planes used are shown in Fig. 1. From the respective scans the

mean values, as well as the cardiac waveforms, of the following flows were assessed: (1) arterial blood flow in the internal carotid (ICAs) and vertebral arteries (VAs), and venous flow in the internal jugular veins (IJVs), (2) CSF flow in the aqueduct, (3) CSF flow at the cervical level. The settings for the three scans (1 / 2 / 3) were: flip angle 15 / 10 / 10°; repetition time 9.6 / 16 / 15 ms; echo time 5.8 / 11 / 10 ms, encoding velocity 70 / 7 / 20 cm/s, and voxel size 0.9×0.9×6 / 1.2×1.2×5 / 1.2×1.2×5 mm^3. The number of signal averages was 2 for all scans. For each sequence, 32 cardiac frames were retrospectively reconstructed with signals acquired from a peripheral pulse detector or ECG. This means that the absolute time resolution of the reconstructed flow waveforms was dependent on the heart rate, while the total number of flow values was the same for all subjects.

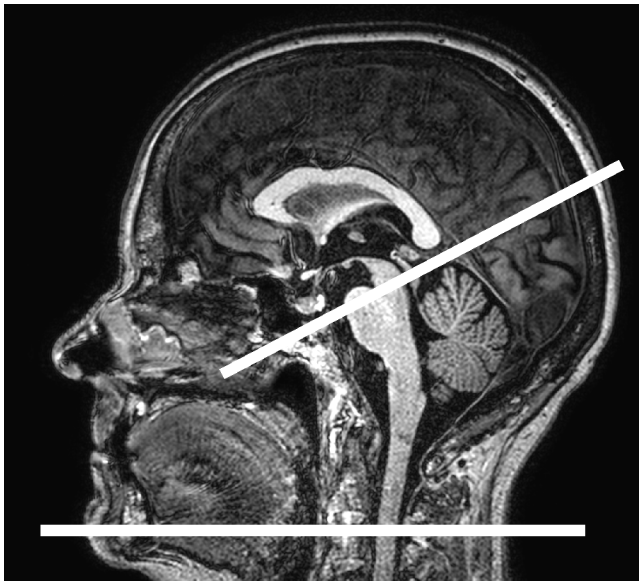

Figure 1. Illustration of the location of phase contrast MRI imaging planes. Sagittal MRI image showing the location of the PC-MRI imaging planes for blood flow (sequence 1) and cervical CSF flow (sequence 2), placed between the second and third vertebrae (lower line), and for the aqueduct flow (sequence 3), placed at the mid-level of the aqueduct (upper line).

Flow measurements

Flow measurements were performed using the computer software Segment (version 1.9 R2832, http://segment.heiberg.se) (17). A region of interest (ROI) was manually drawn around each vessel or CSF space cross section in the magnitude images of the PC-MRI data. The ROIs were kept constant in location, size and shape over the cardiac cycle and were drawn to include the entire cross section where flow occurred at any part of the cardiac cycle. Additional ROIs were drawn in stationary surrounding tissue for manual background phase correction. All ROIs were drawn by the same operator.

The 32 corrected mean velocity values of each measurement ROI were multiplied with the ROI area to determine the flow waveform over the cardiac cycle. By convention, arterial and CSF

flow was labeled as positive when in the cranial direction, whereas venous flow was labeled as positive when in the caudal direction. The flow in the left and right ICAs were added in each individual to determine the ICA flow; the ICA flow was also added to the flow in the left and right VAs, to determine the total cerebral blood flow (tCBF). The flow in the left and right IJVs was also summed and used for calculations of the cerebral venous outflow.

Flow parameters

Net flow was defined as the mean flow over the cardiac cycle, i.e. the average flow during the entire PC-MRI acquisition. Note that, similarly to most PC-MRI studies, we do not present net flow for the cervical CSF space, as the very low flow and the relatively large size of the ROI makes the net flow value very susceptible to noise. Pulsatility index (PI) was calculated for tCBF as described in Fig. 2A (18), and stroke volume (SV, all flows) as in Fig. 2B-C (19). In addition to blood and CSF waveforms, SV was determined for the difference of the arterial and venous waveform, which was defined as arteriovenous SV (13,20), the sum of the arterial and cervical CSF waveform, defined as arteriocervical SV (21), and the sum of the arteriovenous and cervical CSF waveform, defined as intracranial SV (22). E.g. the arteriovenous waveform was calculated by subtracting the venous flow from the tCBF at each of the 32 cardiac frames, before carrying out the SV calculation as described in Fig. 2B-C. Given that the entire cerebral venous outflow does not pass through the IJVs, the measured flow was rescaled so that the venous net flow was equal to the tCBF in the calculation of the combined stroke volumes (1,23) (the presented IJV values are not scaled). In addition to net aqueduct flow (calculated as above), the parameter called “average total aqueduct flow” was analyzed; it was calculated according to the definition given by Luetmer et. al. (5) as mean of the absolute values of flow over the cardiac cycle.

Average waveforms of blood and CSF flows in healthy and INPH, respectively, were also determined. The waveforms were first synchronized between individuals (with respect to the starting point of the waveform) in order to compensate for any variability in the cardiac gating (e.g. due to gating with peripheral pulse detector or ECG). Synchronization was based on identification of the cardiac segment with the steepest rise of the tCBF waveform for each individual; this was designated as the first cardiac frame. After synchronization of the starting frame, the mean value and corresponding confidence interval was calculated at each cardiac cycle frame, resulting in 32 data points for each average waveform (the same number as for each reconstructed individual waveform). Thus, the averaging is based on the temporal resolution of the reconstructed PC-MRI data, which is in relation to the duration of the cardiac cycle rather than absolute time units, and the waveforms are presented using a relative time axis (percent of the total cardiac cycle) to reflect this. The same synchronization and averaging was used for all flow waveforms.

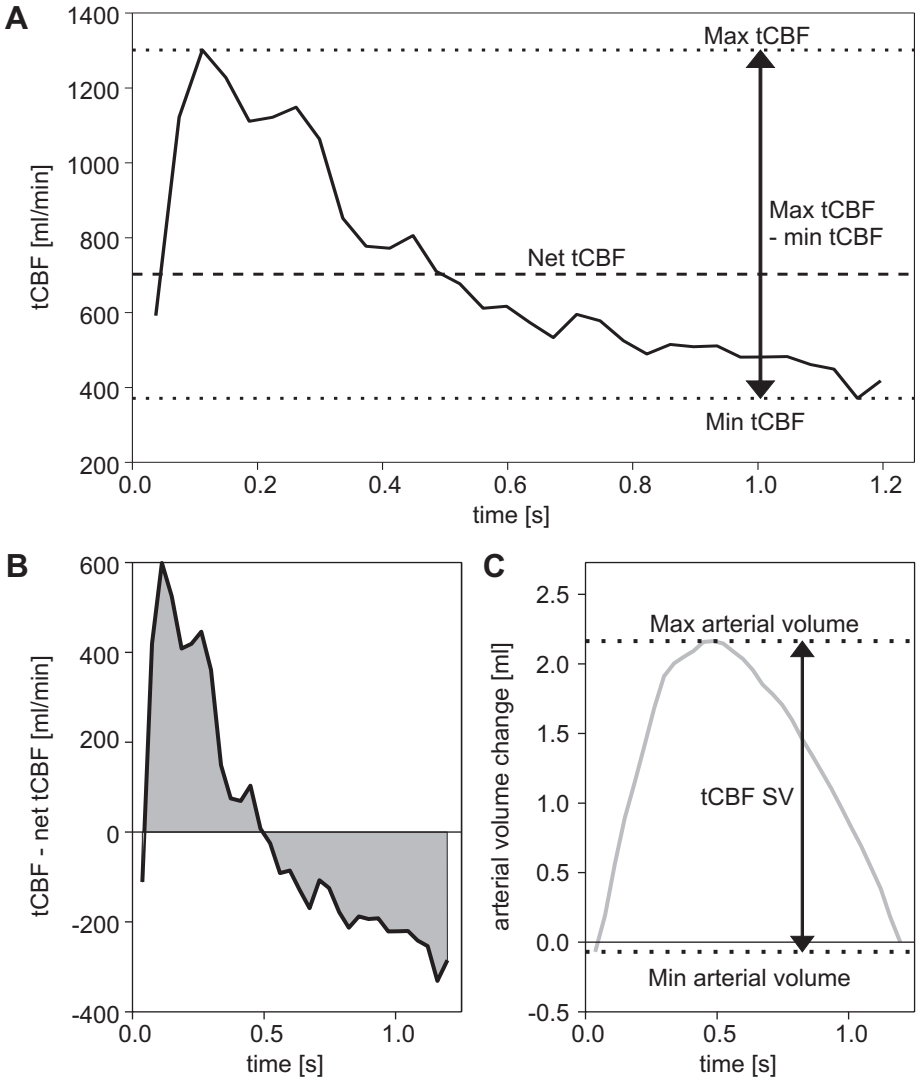

Figure 2. (A-C) Illustration of the calculation of flow parameters. (A) Net total cerebral arterial inflow (tCBF) was the mean flow of the 32 cardiac frames; the tCBF pulsatility index (PI) was the difference between the maximum and minimum tCBF (as indicated by the arrow and dotted lines), divided by the net tCBF (dashed line). (B) The net tCBF was subtracted from the tCBF waveform, and a cumulative integration was performed, i.e. for each cardiac frame the intracranial arterial volume change (shown in C) was the sum of the area under the curve (grey) to the left of that frame (with area under zero having negative values). (C) The tCBF stroke volume (SV) was the difference between the maximum and minimum of the intracranial arterial volume change (as indicated by the arrow and dotted lines).

Temporal delay parameters

The arterial pulse is propagated to venous and CSF flows (24). The delays between different waveforms, e.g. arteriovenous delay (i.e. delay from arterial to venous waveform), were analyzed using cross-correlation, with the sum of the flow waveforms in the ICAs as the reference. The delay was estimated as the lag time [ms] corresponding to the maximum cross-

correlation coefficient. To avoid errors in cases with very low pulsatility, only cases with a correlation maxima above a specified limit were accepted (1 value excluded). To facilitate the setting of this limit so that a low mean flow would not lead to exclusion from the analysis, the cross-correlation coefficient was normalized (each signal was scaled with a constant such that autocorrelation at zero lag = 1). After normalization the highest possible value was 1, and the limit was set to 0.5.

Ventricular volumes

Ventricular volume was estimated by manual segmentation using the software QBrain (v 2.0, Medis Medical Imaging Systems, Leiden, The Netherlands). The method and values for 40 of the healthy subjects have been published previously (25).

Statistics

Statistics were calculated using PASW statistics (version 18, IBM, Armonk, NY). Population characteristics were compared using independent samples Student's t-tests (age and heart rate) or Chi-Square tests (sex). Comparisons between groups were based on multiple linear regression with the tested parameter as the dependent variable, INPH status and sex as a fixed factor predictors, and age as a covariate predictor. The study was designed to match the distributions of age and sex by specifying appropriate inclusion criteria for the healthy, but the inclusion of INPH subjects was only finalized upon classification of all subjects according to the international diagnostic guidelines for INPH, which was performed after the MR investigations were completed. As the proportion of females and males the age distribution was not perfectly matched in the final groups, sex and age variables were included in the regression to ensure that the results could be generalized to larger populations. A post-hoc test was also carried out, comparing the INPH group to a smaller control group, where one healthy subject of the same gender and closest in age was matched to each INPH subject. Levene's test for equality of variances was used to compare variability in the groups, and Fisher's exact test to compare ratios. Correlations were assessed as partial correlation coefficients, correcting for age and sex. Statistical significance was set at $P<0.05$.

Results

Aqueduct CSF flow pulsatility was higher in INPH than in healthy, as illustrated by differences in the average waveform (Fig. 3) and the SV (Table 2). Aqueduct SV and average total aqueduct flow correlated to ventricular volume (Table 3).

The group mean of the net aqueduct CSF flow was directed from the third to the fourth ventricle (caudal direction) for INPH (-0.47 ml/min, $P=0.16$) and healthy (-0.26 ml/min, $P<0.01$), and these values did not differ significantly (Table 2). The reason that the mean value for INPH was not significantly different from zero, while the healthy mean value was, was likely that the

variability was five times higher than in healthy elderly (SD = 1.26 ml/min vs. 0.25 ml/min, P<0.01). Five of the INPH patients (31%) had net aqueduct CSF flow in the cranial direction (fourth to third ventricle), compared to 6 of the healthy subjects (14%).

The cervical CSF SV was significantly lower in INPH than in healthy (Table 2, Fig. 3)).

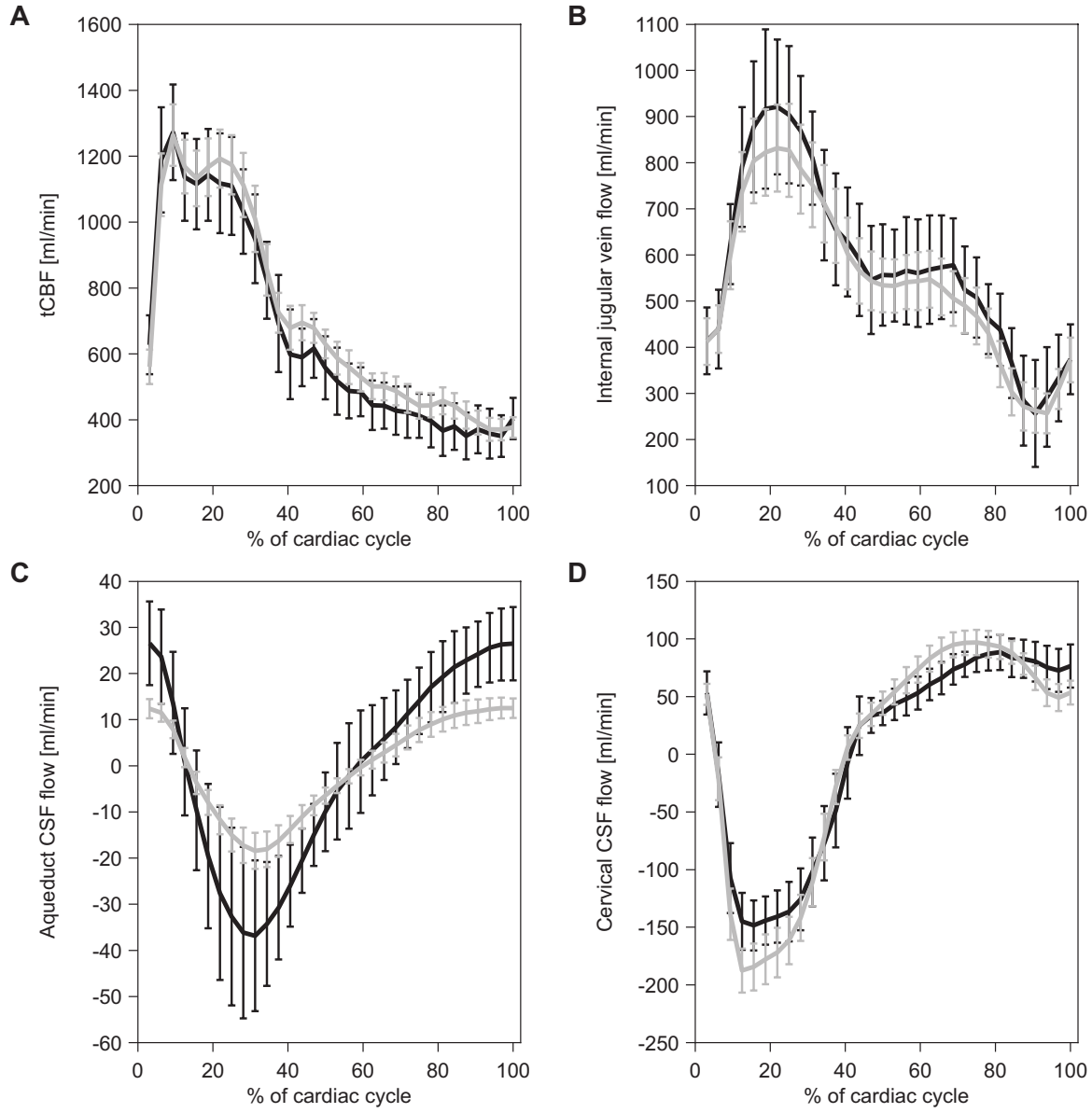

Figure 3. (A-D) Comparison of flow waveforms for healthy elderly and INPH subjects. Average flow waveforms are shown in grey for healthy elderly (N=35), and in black for INPH (N=16). Bars represent the confidence interval of the group means at each of the 32 cardiac frames, where each cardiac frame corresponds to 3.125% of the cardiac cycle (which in turn corresponds to 30±4 ms for healthy and 27±5 ms for INPH subjects (mean±SD), based on PC-MRI sequence 1). (A) tCBF, (B) IJV flow, (C) aqueduct CSF flow (N=33 healthy elderly), and (D) cervical CSF flow (N=14 INPH).

No differences were found in the tCBF (Table 2); analysis of the distributions revealed that 50% of the INPH subjects had tCBF under the 25th percentile of the healthy group, though a small subset of subjects had high tCBF (3 subjects > 90th percentile). The net ICA flow was significantly lower in INPH (Table 2), while the vertebral artery net flow was similar (INPH: 201±95 ml/min vs. healthy: 184±52 ml/min, p=0.45). The cardiac-related waveform of tCBF was similar for the two groups (Fig. 3); no difference was found in tCBF SV or ICA SV (Table 2).

No significant differences were found in the internal jugular vein flow (Table 2, Fig. 3).

The arteriovenous delay was not significantly different between INPH and healthy elderly, nor was any other temporal delay between flow waveforms or any of the combined stroke volumes (Table 2).

The post-hoc test based on the smaller, one-to-one matched healthy elderly group did not affect the results presented above, except that the difference in net ICA flow was not statistically significant (P=0.15, the mean for the healthy decreased from 519 to 507 ml/min). Differences in the mean values for the total (N=35) and small (N=16) control groups were less than 10%, with the exception of the flow delays, which increased by approximately 5 ms, and the measures of aqueduct pulsatility, where aqueduct SV decreased by 15 µl and average total aqueduct flow by 1 ml/min.

Discussion

This study compared blood and CSF flow, including pulsatility, between INPH and healthy elderly. Our results showed that INPH was characterized by higher aqueduct CSF pulsatility, lower cervical CSF pulsatility and a higher variability in the net aqueduct CSF flow in INPH. The majority of the INPH subjects had net flow of CSF directed from the lateral and third ventricles to the fourth ventricle (caudal flow). Net blood flow in the ICA was lower in INPH, though the tCBF was not different.

Flow and pulsatility of the CSF

Our findings regarding the direction of net aqueduct CSF flow contradict previous studies (1,11,12,14). In contrast to those, we used a rigorous inclusion process with two independent reviewers for confirming the INPH diagnosis, and age-matched controls. Inclusion criteria of one of the previous studies was a mix of idiopathic and secondary NPH, as well as hyperdynamic aqueduct flow (1). Two others did not specify the cause of communicating hydrocephalus (11,14), and a fourth used only two control subjects (12). The highest net aqueduct CSF flow magnitudes observed in this study, both in and out of the third ventricle, were found in the INPH group. It is important to note that it has been shown that aqueduct CSF flow varies with the respiratory cycle (26), and it may also vary with other slower variations in

ICP, e.g. due to cerebral autoregulation. Recent publications have emphasized that ICP and other parameters assessed during CSF infusion studies vary with time (27,28), and likely this also applies to CSF flow measurements. The variability of repeated PC-MRI measurements of net aqueduct CSF flow, in the same subject, is as large as the variability between subjects, in healthy individuals (19). This phenomenon was probably magnified in INPH, causing the higher variability. In spite of this, our results showed a trend towards caudal flow in INPH and suggest that retrograde net flow is not a typical characteristic of INPH. All together, these observations strongly indicate that single PC-MRI measurements of net aqueduct CSF flow can be highly variable, and should not be used to guide clinical decisions in INPH.

Our results confirm that the aqueduct CSF pulsatility is higher in INPH than in healthy elderly (1–6). The correlation between ventricular volume and aqueduct stroke volume suggests that the increased aqueduct CSF pulsatility may largely reflect the ventriculomegaly in INPH. Ringstad et al previously described a similar finding, i.e., stroke volume was correlated to ventricular volume (8). Similarly, the reduced pulsatility of the cervical CSF, in agreement with some previous findings (3) but in contradiction to others (1,13), may reflect an overall redistribution of the intracranial CSF volume, as it has been suggested that the supratentorial subarachnoid space may be reduced in INPH, as part of the so-called DeSH sign (29,30). I.e., with less total volume of CSF in the supratentorial subarachnoid space the pulsatile flow of CSF from this space may be reduced by a larger amount than the pulsatile flow through the aqueduct is increased, resulting in less pulsatile flow at the cervical level.

The average CSF flow waveforms presented here are similar to previous findings for healthy elderly (31,32) and communicating hydrocephalus (1). However, some previous studies have shown reduced cervical CSF flow delays (1,13), which we did not find in the present study.

Blood flow and pulsatility

The net ICA flow was lower in INPH, though the statistical significance of this difference did not persist in the post-hoc test, potentially due to reduced power. Lower flow in the anterior circulation is in agreement with INPH perfusion studies showing frontal hypoperfusion (33). Other findings regarding blood flow in this study were less distinct; there was no difference in tCBF or tCBF SV between INPH and controls, and no reduction of flow delays in INPH. Previous PC-MRI studies regarding blood flow have been contradictory, showing both reduced (1,2) and normal (13) tCBF in INPH, but generally reduced flow delays (1,2,13). An interesting hypothesis regarding INPH pathophysiology is “pulse wave encephalopathy”. While we found no alteration in blood flow pulsatility, we only measured pulsatility in the large arteries (carotids and vertebrals) and confirmation of this theory is only possible if pulsatility is measured along the vascular tree, including distal branches (34).

Potential implications regarding craniospinal compliance

We found that the pulsatility of CSF flow was reduced at the cervical level in INPH, while it was increased in the aqueduct. Greitz et. al. suggested that this finding indicates reduced arterial compliance (3), based on previous findings indicating that cervical CSF pulsatility reflects arterial expansion, while aqueduct pulsatility reflects capillary expansion (36). If the former decreased due to arterial stiffening, the latter would increase due to impaired pulsatile dampening via the Windkessel mechanism. By contrast, arterial stroke volume (tCBF SV), as we measured and found to be unaltered in INPH, should reflect the total downstream expansion, i.e. the sum of arterial and capillary expansion, and does not indicate where the expansion occurs.

Miyati et al. found a reduction of the PC-MRI-based intracranial compliance index (37) in INPH compared to healthy, related to a reduced intracranial volume change (by ~50%) in INPH (38). In line with these findings, we observed a trend toward reduced intracranial SV (~20%) in INPH compared to healthy elderly (P=0.08). One could also speculate that the reduced cervical CSF pulsatility we observed in INPH may be caused by reduced *spinal* compliance, though most of the focus on compliance in INPH research has been aimed toward the intracranial compartment. Previously, reduced flow delays have also been interpreted as an indication of reduced intracranial or arterial compliance in INPH (1,2,13), but none of the flow delays were significantly altered in INPH in the present study. Thus, our results are not conclusive regarding a potential reduction of craniospinal compliance in INPH.

Limitations

Our study employed a higher encoding velocity than previous studies of aqueduct CSF net flow (1,11,12), which may explain some of the difference in the results. Some improvement in the reliability of this type of measurement may be achieved using PC-MR sequences with multipoint velocity encoding (39). To provide a definitive answer as to whether the reversed CSF circulation is a component of the INPH pathophysiology, an alternative measurement technique is likely needed, e.g. based on several repeated measurements or a long duration measurement.

In general, our CSF stroke volumes are somewhat higher, while our flow delays are somewhat lower, than those presented in the literature (20,40,31). This emphasizes that differences in spatial and time resolution, V_{enc}, and even the approach to drawing the ROI, are important for the magnitude of such values. We used manual ROI delineation in this study, with an approach of being generous rather than conservative in size, which could explain some of the differences. With manual delineation a certain inter-operator variability is inherent, but importantly all ROI for both groups were drawn by the same operator, and then verified (in a single frame) by a second, experienced operator. For the aqueduct measurements in particular, the spatial resolution of the PC-MRI sequence used was relatively low, which may lead to overestimation

of the aqueduct area and SV due to partial volume effects (19). Such overestimation is larger for smaller aqueducts, and thus this may have reduced the observed difference in SV between healthy elderly and INPH. The values of normal aqueduct SV presented in this study should thus be adjusted if comparisons are to be made with higher resolution PC-MRI measurements, and indeed use of the this normal material in general should not be undertaken without careful consideration of differences in the PC-MRI sequences.

In the calculation of the combined stroke volumes, we employed scaling of the IJV flow waveform to match the mean to the net tCBF to provide an estimate of the total venous outflow. This assumes that the flow waveform of other draining veins is the same as the IJV waveform, which may not be the case, and may thus obscure any difference in the non-IJV venous flow between healthy elderly and INPH. Additionally, as discussed above regarding the net CSF flows, slow variations in intracranial blood volume may mean that the in- and outflow of blood to the cranium may not be absolutely equal for the duration of the PC-MRI sequence.

While we identified a positive correlation between ventricular volume and aqueduct stroke volume, it was not exceptionally high, and no causal relationship has been established. Future research should thus address whether the increase in aqueduct CSF flow pulsatility plays an active part in the INPH pathophysiology, or if it is simply an effect of the increased volume of CSF and larger surface area of the ventricular system. If aqueduct flow does play an active role, clarifying what mechanism may instigate the phenomenon may offer new avenues for treatment and outcome prediction.

Conclusion

The main characteristic of the flow of blood and CSF in INPH was increased pulsatility of the aqueduct CSF flow; additionally, the CSF flow pulsatility at the cervical level was reduced, as was the net ICA blood flow. The majority of the INPH subjects had net aqueduct CSF flow in the normal direction, i.e. out of the third ventricle, rather than into the ventricles, as previously suggested. Our findings do not support the use of a single measurement of net aqueduct CSF flow as a guide for clinical decisions in INPH. The changes in CSF flow pulsatility may reflect the altered distribution of intracranial CSF volume in INPH, but the causality of this relationship is unclear.

Conflict of Interest and Sources of Funding Statement

The authors declare that they have no competing interests. This project was financed by the Swedish Research Council (grant number 221-2011-5216).

Acknowledgements

The authors have no acknowledgements.

References

1 BALÉDENT O, GONDRY-JOUET C, MEYER M-E et al. Relationship Between Cerebrospinal Fluid and Blood Dynamics in Healthy Volunteers and Patients with Communicating Hydrocephalus. Invest Radiol 2004;**39**:45–55.

2 BATEMAN GA, LOISELLE AM. Can MR measurement of intracranial hydrodynamics and compliance differentiate which patient with idiopathic normal pressure hydrocephalus will improve following shunt insertion? Acta Neurochir (Wien) 2007;**149**:455–62.

3 GREITZ D, HANNERZ J, RÄHN T, BOLANDER H, ERICSSON A. MR imaging of cerebrospinal fluid dynamics in health and disease. On the vascular pathogenesis of communicating hydrocephalus and benign intracranial hypertension. Acta radiol 1994;**35**:204–11.

4 GIDEON P, STÅHLBERG F, THOMSEN C, GJERRIS F, SØRENSEN PS, HENRIKSEN O. Cerebrospinal fluid flow and production in patients with normal pressure hydrocephalus studied by MRI. Neuroradiology 1994;**36**:210–5.

5 LUETMER PH, HUSTON J, FRIEDMAN JA et al. Measurement of cerebrospinal fluid flow at the cerebral aqueduct by use of phase-contrast magnetic resonance imaging: technique validation and utility in diagnosing idiopathic normal pressure hydrocephalus. Neurosurgery 2002;**50**:534–43.

6 MIYATI T, MASE M, BANNO T et al. Frequency analyses of CSF flow on cine MRI in normal pressure hydrocephalus. Eur Radiol 2003;**13**:1019–24.

7 GREITZ D. Radiological assessment of hydrocephalus: new theories and implications for therapy. Neurosurg Rev 2004;**27**:145–65.

8 RINGSTAD G, EMBLEM KE, GEIER O, ALPERIN N, EIDE PK. Aqueductal Stroke Volume: Comparisons with Intracranial Pressure Scores in Idiopathic Normal Pressure Hydrocephalus. AJNR Am J Neuroradiol 2015. doi: 10.3174/ajnr.A4340. [Epub ahead of print].

9 MARMAROU A, BERGSNEIDER M, KLINGE PM, RELKIN NR, BLACK PM. The Value of Supplemental Prognostic Tests for the Preoperative Assessment of Idiopathic Normal-Pressure Hydrocephalus. Neurosurgery 2005;**57**:S2: 17–28.

10 VANNESTE JAL. Diagnosis and management of normal-pressure hydrocephalus. J Neurol 2000;**247**:5–14.

11 PENN RD, BASATI S, SWEETMAN B, GUO X, LINNINGER AA. Ventricle wall movements and cerebrospinal fluid flow in hydrocephalus. J Neurosurg 2011;**115**:1–6.

12 RINGSTAD G, EMBLEM KE, EIDE PK. Phase-contrast magnetic resonance imaging reveals net retrograde aqueductal flow in idiopathic normal pressure hydrocephalus. J Neurosurg 2015. doi: 10.3171/2015.6.JNS15496. [Epub ahead of print].

13 ELSANKARI S, GONDRY-JOUET C, FICHTEN A et al. Cerebrospinal fluid and blood flow in mild cognitive impairment and Alzheimer's disease: a differential diagnosis from idiopathic normal pressure hydrocephalus. Fluids Barriers CNS 2011;**8**:12.

14 KIM DS, CHOI JU, HUH R, YUN PH, KIM DI. Quantitative assessment of cerebrospinal fluid hydrodynamics using a phase-contrast cine MR image in hydrocephalus. Childs Nerv Syst 1999;**15**:461–7.

15 RELKIN NR, MARMAROU A, KLINGE PM, BERGSNEIDER M, BLACK PM. Diagnosing Idiopathic Normal-Pressure Hydrocephalus. Neurosurgery 2005;**57**:S2: 4–16.

16 MALM J, JACOBSSON J, BIRGANDER R, EKLUND A. Reference values for CSF outflow resistance and intracranial pressure in healthy elderly. Neurology 2011;**76**:903–9.

17 HEIBERG E, SJÖGREN J, UGANDER M, CARLSSON M, ENGBLOM H, ARHEDEN H. Design and validation of Segment--freely available software for cardiovascular image analysis. BMC Med Imaging 2010;**10**:1.

18 GOSLING RG, KING DH. Arterial Assessment by Doppler-shift Ultrasound. Proc R Soc Med 1974;**67**:447–9.

19 WÅHLIN A, AMBARKI K, HAUKSSON J, BIRGANDER R, MALM J, EKLUND A. Phase contrast MRI quantification of pulsatile volumes of brain arteries, veins, and cerebrospinal fluids compartments: Repeatability and physiological interactions. J Magn Reson Imaging 2011;**c**:1–8.

20 BALÉDENT O, HENRY-FEUGEAS M-CC, IDY-PERETTI I. Cerebrospinal Fluid Dynamics and Relation with Blood Flow. A Magnetic Resonance Study with Semiautomated Cerebrospinal Fluid Segmentation. Invest Radiol 2001;**36**:368–77.

21 WÅHLIN A, AMBARKI K, BIRGANDER R, ALPERIN N, MALM J, EKLUND A. Assessment of craniospinal pressure-volume indices. AJNR Am J Neuroradiol 2010;**31**:1645–50.

22 BALÉDENT O, FIN L, KHUOY L et al. Brain Hydrodynamics Study by Phase-Contrast Magnetic Resonance Imaging and Transcranial Color Doppler. J Magn Reson Imaging 2006;**24**:995–1004.

23 ENZMANN DR, PELC NJ. Cerebrospinal fluid flow measured by phase-contrast cine MR. AJNR Am J Neuroradiol 1993;**14**:1301–7.

24 BHADELIA RA, BOGDAN AR, WOLPERT SM. Analysis of cerebrospinal fluid flow waveforms with gated phase-contrast MR velocity measurements. AJNR Am J Neuroradiol 1995;**16**:389–400.

25 AMBARKI K, ISRAELSSON H, WÅHLIN A, BIRGANDER R, EKLUND A, MALM J. Brain ventricular size in healthy elderly: comparison between Evans index and volume measurement. Neurosurgery 2010;**67**:94–9.

26 CHEN L, BECKETT A, VERMA A, FEINBERG D A. Dynamics of respiratory and cardiac CSF motion revealed with real-time simultaneous multi-slice EPI velocity phase contrast imaging. Neuroimage 2015;**122**:281–7.

27 SWALLOW DMA, FELLNER N, VARSOS G V. et al. Repeatability of cerebrospinal fluid constant rate infusion study. Acta Neurol Scand 2014;**130**:131–8.

28 KASPROWICZ M, LALOU DA, CZOSNYKA M, GARNETT M, CZOSNYKA Z. Intracranial pressure, its components and cerebrospinal fluid pressure-volume compensation. Acta Neurol Scand 2015;:1–13.

29 KITAGAKI H, MORI E, ISHII K, YAMAJI S, HIRONO N, IMAMURA T. CSF spaces in idiopathic normal pressure hydrocephalus: morphology and volumetry. AJNR Am J Neuroradiol 1998;**19**:1277–84.

30 HASHIMOTO M, ISHIKAWA M, MORI E, KUWANA N. Diagnosis of idiopathic normal pressure hydrocephalus is supported by MRI-based scheme: a prospective cohort study. Cerebrospinal Fluid Res 2010;**7**:18.

31 SCHMID DANERS M, KNOBLOCH V, SOELLINGER M et al. Age-specific characteristics and coupling of cerebral arterial inflow and cerebrospinal fluid dynamics. PLoS One 2012;**7**:e37502.

32 STOQUART-ELSANKARI S, BALÉDENT O, GONDRY-JOUET C, MAKKI M, GODEFROY O, MEYER M-E. Aging effects on cerebral blood and cerebrospinal fluid flows. J Cereb Blood Flow Metab 2007;**27**:1563–72.

33 OWLER BK, PICKARD JD. Normal pressure hydrocephalus and cerebral blood flow: a review. Acta Neurol Scand 2001;**104**:325–42.

34 ZARRINKOOB L, AMBARKI K, WAHLIN A et al. Aging alters the dampening of pulsatile blood flow in cerebral arteries. J Cereb Blood Flow Metab 2016. doi: 10.1177/0271678X16629486. [Epub ahead of print].

35 WAGSHUL ME, EIDE PK, MADSEN JR. The pulsating brain: A review of experimental and clinical studies of intracranial pulsatility. Fluids Barriers CNS 2011;**8**:5.

36 GREITZ D, WIRESTAM R, FRANCK A, NORDELL B, THOMSEN C, STÅHLBERG F. Pulsatile brain movement and associated hydrodynamics studied by magnetic resonance phase imaging The Monro-Kellie doctrine revisited. Neuroradiology 1992;**34**:370–80.

37 ALPERIN N, LEE SH, LOTH F, RAKSIN PB, LICHTOR T. MR-Intracranial pressure (ICP): a method to measure intracranial elastance and pressure noninvasively by means of MR imaging: baboon and human study. Radiology 2000;**217**:877–85.

38 MIYATI T, MASE M, KASAI H et al. Noninvasive MRI assessment of intracranial compliance in idiopathic normal pressure hydrocephalus. J Magn Reson Imaging 2007;**26**:274–8.

39 KNOBLOCH V, BINTER C, KURTCUOGLU V, KOZERKE S. Arterial, venous, and cerebrospinal fluid flow: simultaneous assessment with Bayesian multipoint velocity-encoded MR imaging. Radiology 2014;**270**:566–73.

40 YIALLOUROU TI, DANERS MS, KURTCUOGLU V et al. Continuous positive airway pressure alters cranial blood flow and cerebrospinal fluid dynamics at the craniovertebral junction. Interdiscip Neurosurg 2015;**2**:152–9.